Molecular Dissection of the 5′ Region of *no-on-transientA* of *Drosophila melanogaster* Reveals *cis*-Regulation by Adjacent *dGpi1* Sequences

Federica Sandrelli,* Susanna Campesan,† Maria Giovanna Rossetto,* Clara Benna,* Emanuela Zieger,* Aram Megighian,‡ Martin Couchman,†,[1] Charalambos P. Kyriacou† and Rodolfo Costa*

**Dipartimento di Biologia, Università di Padova, 35131 Padova, Italy, †Department of Genetics, University of Leicester, Leicester LE1 7RH, England and ‡Dipartimento di Anatomia e Fisiologia Umana, Università di Padova, 35131 Padova, Italy*

Manuscript received May 1, 2000
Accepted for publication October 23, 2000

ABSTRACT

The *nonA* gene of *Drosophila melanogaster* is important for normal vision, courtship song, and viability and lies ~350 bp downstream of the *dGpi1* gene. Full rescue of *nonA* mutant phenotypes can be achieved by transformation with a genomic clone that carries ~2 kb of 5′ regulatory material and that encodes most of the coding sequence of *dGpi1*. We have analyzed this 5′ region by making a series of deleted fragments, fusing them to yeast *GAL4* sequences, and driving *UAS-nonA* expression in a mutant *nonA* background. Regions that both silence and enhance developmental tissue-specific expression of *nonA* and that are necessary for generating optomotor visual responses are identified. Some of these overlap the *dGpi1* sequences, revealing *cis*-regulation by neighboring gene sequences. The largest 5′ fragment was unable to rescue the normal electroretinogram (ERG) consistently, and no rescue at all was observed for the courtship song phenotype. We suggest that sequences within the *nonA* introns that were missing in the *UAS-nonA* cDNA may carry enhancer elements for these two phenotypes. Finally, we speculate on the striking observation that some of the *cis*-regulatory regions of *nonA* appear to be embedded within the coding regions of *dGpi1*.

THE sex-linked *no-on-transientA* (*nonA*) gene in Drosophila encodes a putative RNA-binding protein (Jones and Rubin 1990), and mutations in this gene affect viability (Stanewsky *et al.* 1993), visual behavior (Hotta and Benzer 1969), and the male fly's courtship song (Kulkarni *et al.* 1988). The *nonA* transcript is present in the fertilized egg, but at a more advanced developmental stage its expression seems to decrease in all tissues except in the central nervous system (CNS), where it starts to decline only toward the end of embryonic development (Rendahl *et al.* 1992). The expression pattern of the NONA protein is similar, but not identical, to that of its RNA. The protein seems to be present ubiquitously in the developing oocyte and the embryonic, larval, pupal, and adult stages. The protein is localized in the cytoplasm of the fertilized egg, but it enters the nuclei at the cellular blastoderm stage and remains nuclear in most tissues during embryonic and adult development (Frash and Saumweber 1989; Rendahl *et al.* 1992). Besser *et al.* (1990) also showed that the NONA protein is localized in several puffs on polytene chromosomes of Drosophila larvae, and its binding seemed correlated with active transcription within these puffs (Frash and Saumweber 1989). However, evidence for any specific *in vivo* role for NONA is equivocal (Reim *et al.* 1999).

Despite NONA's almost ubiquitous adult expression pattern, mutations in the gene have specific effects on behavior. The first *nonA* mutants were isolated in screens for flies defective in phototaxis, were subsequently shown to lack both light-on and light-off transient spikes in the electroretinogram (ERG), and were impaired in their optomotor responses (Hotta and Benzer 1969; Pak *et al.* 1970; Heisenberg 1972; Heisenberg and Gotz 1975). In a screen for defective courtship songs, the $nonA^{diss}$ mutant was identified by its abnormal pulse songs, which become increasingly polycyclic and very high in amplitude during a song burst (Kulkarni *et al.* 1988). Extensive mutational analysis of various domains of *nonA* have revealed that if a coding region mutation affects the song phenotype, then vision is always affected, but not vice versa, suggesting that the visual pathway is more sensitive to NONA disruption (Rendahl *et al.* 1992, 1996; Stanewsky *et al.* 1996).

The phenotypic effects caused by an amorphic allele of the *nonA* locus have been studied by generating an X-linked deletion, *T(1;4)9e2-10*, which removed both *nonA* and the distal, partially overlapping, lethal locus *l(1)i19e* (Jones and Rubin 1990). Viable $nonA^{-}$ mutants

Corresponding author: Rodolfo Costa, Dipartimento di Biologia, Università di Padova, Via U. Bassi 58/B, 35131 Padova, Italy.
E-mail: costa@civ.bio.unipd.it

[1]*Present address:* Department of Biology, Imperial College, Ascot, Berks SL5 7PY, England.

were then generated by transforming flies carrying the *T(1;4)9e2-10* deletion with a clone encoding exclusively for the lethal gene's product (Stanewsky *et al.* 1993). In hemizygous males, deletion of the *nonA* gene causes semilethality as only 10–30% of the expected number eclose from metamorphosis. If kept at a temperature below 25° no $nonA^-$ males emerge. The $nonA^-$ individuals are deficient in locomotor activity and flight and less than one-third of them survive to reproduce. In visual and courtship behavior, $nonA^-$ deficient males show similar, although more severe, defects to those of $nonA^{diss}$ mutants, confirming that $nonA^{diss}$ is indeed the allele closest to an amorphic mutation. $nonA^{diss}$ encodes an arginine-to-cysteine substitution in a region that is rich in charged residues and lies C terminal to the two RNA recognition motif repeats, whereas the visually defective mutations $nonA^{P14}$ and $nonA^{H2}$ map, respectively, in the center of, or just outside, the second RRM repeat (Rendahl *et al.* 1996).

As yet, little is known about the regulatory regions of *nonA*. Here, we describe a series of 5′ deletions that remove progressively more of the sequences of a gene called *dGpi1*, which has been recently identified within the *nonA* promoter region and which almost certainly corresponds to the vital gene *l(1)i19e* (Jones and Rubin 1990; Campesan *et al.* 2001, accompanying article). *dGpi1* lies 325 bp 5′ to the *nonA* transcription start and encodes a component used in the biosynthesis of glycosylphosphatidylinositol, which is used to anchor eukaryotic proteins to membranes (Campesan *et al.* 2001, accompanying article). The *nonA* promoter fragments were fused to the yeast transcriptional activator *gal4* (Fischer *et al.* 1988) and used to drive *UAS-nonA* expression in a *nonA* mutant background. By comparing wild-type $nonA^+$ and the transformants' developmental expression patterns, visual, and sexual behavior, we have correlated regions of the promoter, including sequences within *dGpi1*, with NONA function.

MATERIALS AND METHODS

Fly stocks: Flies were raised on a standard yeast-glucose-agar medium (Roberts and Standen 1998) and were maintained at 25°, 70% relative humidity, in 12-hr light/12-hr dark cycles. Adults were collected using CO_2 anesthesia. Canton-S was used as the wild-type strain, and the dominantly marked, multiply inverted balancer chromosomes *In(1)FM7, w; In (2LR)O, Cy/Sco* and *w; In(3LR)Ubx130/Tp(3;3)MKRS* stocks were used for determining the chromosomal locations of the different transgenes and for subsequent manipulations of the transgenic lines prior to their analysis (Lindsley and Zimm 1992). Three independent, cytoplasmically expressing β-galactosidase *UAS-lacZ* lines (1025, 1026, and 1027, a gift from A. Brand) were used for the expression studies (Phelps and Brand 1998). The stock $nonA^{diss}$ *f* was originally received from J. Hall, Brandeis University, in 1994. Mutants were repeatedly outcrossed to Canton-S, and the song phenotype re-extracted via the closely linked *forked* bristle marker. This line, called $nonA^{diss}$ *f* (a), provided the mutant background for analyzing the different *KpnGAL4-UASnonA* constructs with respect to the attempted rescue of the courtship song phenotype. The original $nonA^{diss}$ *f* line, called $nonA^{diss}$ *f* (b), provided the mutant background for the attempted rescue of the ERG and optomotor responses. The *T(1:4)9e2-10/In(1) FM7* balanced strain carries a reciprocal translocation *T(1:4)* that uncovers the *nonA* gene and the adjacent essential locus *l(1)i19e* (Stanewsky *et al.* 1993). Females crossed to males carrying an autosomal insertion of the *Drosophila melanogaster* transgene *P[(ry) 235R11]*, which encodes wild-type sequences for both *nonA* and *l(1)i19e* (Jones and Rubin 1990; Stanewsky *et al.* 1993), will generate viable F_1 males. These male transformants were used as suitable $nonA^+$ controls for the courtship song study.

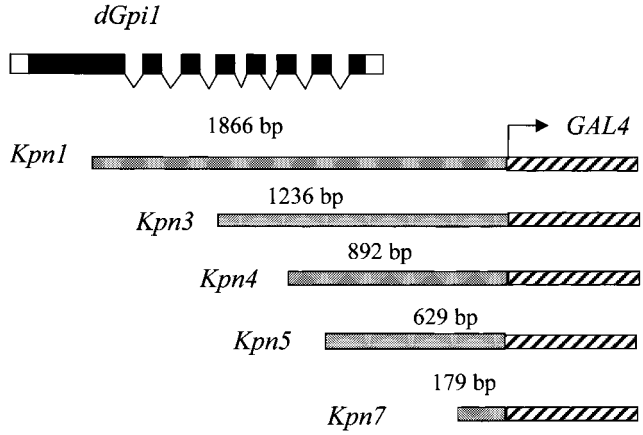

Figure 1.—Schematic representation of the various *nonA* promoter-*GAL4* fusion constructs showing them in relation to the intron-exon structure of the *dGpi1* gene. The 3′ end of each Kpn fragment ends 45 bp downstream of the transcription start of *nonA* and 44 bp upstream of the *nonA* initiating methionine codon (Campesan *et al.* 2001, accompanying article).

Generation of *nonA* promoter-*GAL4* fusions (*KpnGAL4*): Five 5′ progressively deleted fragments of the *D. melanogaster nonA* regulatory region were obtained by PCR amplification, fused with the yeast *GAL4* gene, and cloned into *P*-element transformation vectors. Diagrams of the various gene fusions are shown in Figure 1. This was done by using six primers, one 3′, and five 5′, designed on the basis of the *nonA* sequence published by Jones and Rubin (1990). The primers introduced the restriction sites for *Kpn*I and *Bam*HI at the 5′ termini of the 5′ primers and 3′ primer, respectively. Initially, a 1866-bp region immediately upstream of the coding region of *nonA*, and known to contain the promoter and all the enhancers required for the correct expression of the NONA protein (Jones and Rubin 1990), was amplified via PCR employing the 5′ *Kpn*I primer 5′-GCG**GGTACC**TCTAGACTGAATCAACCA-3′ (positions 1–18 in sequence of Jones and Rubin 1990; boldface represents the restriction site), and the 3′ *Bam*HI primer 5′-TAT**GGATCC**GCTACAACTCGTTGACAA-3′ (positions 1849–1866) with Vent-recombinant DNA polymerase (New England Biolabs, Beverly, MA). The 3′ end of this fragment ends 44 bp upstream of the initiating methionine of *nonA* and 45 bp downstream of the transcription start of *nonA* (Campesan *et al.* 2001, accompanying article). The *nonA 235R11* fragment (Jones and Rubin 1990) was used as the DNA template. The 1866-bp region was cloned as a *Kpn*I-*Bam*HI fragment in front of the *GAL4* gene in the pGATB construct (Brand and Perrimon 1993) to generate *Kpn1*-pGATB. The *Kpn1GAL4* fragment was excised from *Kpn1*-pGATB as a *Kpn*I-*Not*I fragment and subcloned into pW8ΔB,

a pW8 vector (Klemenz *et al.* 1987) in which the *Bam*HI site had been previously deleted following the filling recessed 3′ termini method (Sambrook *et al.* 1989) to generate the transgene we call *Kpn1GAL4*.

A similar procedure was used to amplify a 1236-bp fragment using primer 5′-GCG**GGTACC**ACTACAGATTTCATTGAA-3′ (630–648, 5′ Kpn3), a 892-bp fragment using primer 5′-GC G**GGTACC**CAGGTCGCACTGAGTCCC-3′ (974–991, 5′ Kpn4), a 629-bp fragment using primer 5′-GCG**GGTACC**TATTAA GAGGATGTCATG-3′ (1237–1255, 5′ Kpn5), and a 179-bp fragment using primer 5′-GCG**GGTACC**AGCAAGCTATATT CGACA-3′ (1687–1704, 5′ Kpn7) together with the 3′ *Bam*HI primer, using *Kpn1*pGATB as the template. The relevant Kpn region was then subcloned as a *Kpn*I-*Bam*HI fragment in front of the *GAL4* gene in the pW8ΔB vector to generate the transgenes *Kpn3GAL4*, *Kpn4GAL4*, *Kpn5GAL4*, and *Kpn7GAL4*. All Kpn fragments were automatically sequenced (Turbo Catalyst, Perkin-Elmer, Norwalk, CT) to check for errors.

Generation of *UAS-nonA*: The full-length 3.7-kb *nonA* cDNA was excised from the Bj6-7 clone (Besser *et al.* 1990) as a *Not*I-*Kpn*I and subcloned downstream of the five UAS repeats in the pUAST construct (Brand and Perrimon 1993). This clone has ~1.2 kb of 3′ material downstream of the *nonA* translational stop and includes at least two polyadenylation signals (Besser *et al.* 1990).

Generation of transgenic lines: Transgenic lines were generated by injection of DNA into embryos of strain *y, w; +/+; Sb, e, PΔ 2-3/TM6, Ubx* at a concentration of 600 ng/μl using standard procedures (Rubin and Spradling 1982; Spradling and Rubin 1982). Three independently derived lines (21A, 28A, and 30G) were obtained for *Kpn1GAL4*, two (15A and 19G) for *Kpn3GAL4*, four (5C, 9A, 10D, and 18D) for *Kpn4GAL4*, two (15B and 41B) for *Kpn5GAL4*, three (15E, 24B, and 34A) for *Kpn7GAL4*, and three (9A, 20B, and 21C) for *UAS-nonA*. For each line the chromosomal position of the insert(s) was determined with standard genetic crosses, and all inserts were balanced with dominantly marked, multiple inverted chromosomes. *In situ* hybridization on third instar salivary gland chromosomes was used to pinpoint the map position and to detect the number of inserts in each line using *Kpn1GAL4* and *nonA* cDNA probes and the Boehringer Mannheim (Indianapolis) DIG-DNA labeling and detection kit (Schmidt *et al.* 1988). Each line was checked for the integrity of the transgene by using a single-fly PCR method (Gloor and Engels 1990), employing the 5′ primers reported above and the 3′ primer 5′-TCAGACACTTGGCGCACTTCG-3′ that was designed on the basis of the *GAL4* sequence (GenBank accession no. K01486; Laughon *et al.* 1984). Transgenic lines carrying single insertions on the autosomes were used for subsequent experiments.

Expression analysis: The different homozygous lines transgenic for *Kpn1GAL4*, *Kpn5GAL4*, and *Kpn7GAL4* were crossed to three independent homozygous *UAS-lacZ* lines (1025, 1026, and 1027), whereas the *Kpn3GAL4* and *Kpn4GAL4* lines were crossed only to line 1026. The progeny from each cross were examined for β-galactosidase expression at different developmental stages. At least 30 adults and larvae and 50 embryos were examined for each *Kpn1-7GAL4* and *UAS-lacZ* combination. Three observers evaluated the slides and noted the presence or absence of the blue signal in the various anatomical structures and also recorded the comparative levels of signal (weak or strong).

Immunochemistry and X-gal staining: Embryos were dechorionated and devitellinized as described in Tautz and Pfeifle (1989) and incubated for 2 hr at room temperature in a 1:4000 dilution of mouse anti-β-galactosidase antibody (Boehringer Mannheim). After washing in PBS, embryos were incubated for 1 hr at 37° in a 1:10 dilution of FITC-conjugated goat anti-mouse antibody (Boehringer Mannheim). Embryos were rinsed in PBS and mounted in an antifade solution (Johnson and Nogueira-Araujo 1981) containing 0.05 mg/ml Hoechst 33258 (Sigma, St. Louis). The developmental stages are estimated according to Campos-Ortega and Hartenstein (1985). Third-instar larval brains, larval imaginal discs, and adult female ovaries were dissected in PBS. Whole adults were embedded and frozen in Tissue Tek and sectioned at a thickness of 12 μm with a cryostat. The dissected organs and sectioned materials were fixed for 15 and 5 min, respectively, in 1% glutaraldehyde. After washing in PBS, the different tissues were incubated at 37° in a solution of 10 mm PBS, 150 mm NaCl, 2 mm $MgCl_2$, 3 mm $K_4Fe(CN_6)$, and 3 mm $K_3Fe(CN_6)$ containing a 1:50 dilution of X-gal (25 mg/ml in dimethyl formamide). The time of incubation in staining solution varied for different organs: 1 hr for larval organs, 1.5 hr for female ovaries, and 2 hr for sections. After washing in PBS, they were mounted in 80% glycerol. Ovarian developmental stages are estimated according to King (1970).

Immunocytochemistry of NONA protein: Embryos and adults from the Canton-S strain were used as positive controls and were stained with a mouse anti-NONA antibody (a gift from K. Rendahl) essentially as described in Rendahl *et al.* (1992). They were then incubated overnight at 4° in a solution of primary anti-NONA antibody (1:10,000 for embryos and 1:4000 for adult tissues), washed, incubated, rinsed, and mounted as before. Sections were incubated for 2 hr at room temperature in a 1:100 dilution of HRP-conjugated goat anti-mouse antibody (Kirkegaard and Perry Laboratories Inc.). The staining reaction was made by using the Histomark black kit (Kirkegaard and Perry Laboratories Inc.). Slides were rinsed in H_2O and mounted in 80% glycerol.

Behavioral and physiological analyses: The rescue of mutant behavior was examined in $nonA^{diss}$ transgenic males carrying various combinations of *KpnGAL4* and *UAS-nonA in trans* on the second chromosome. These males were obtained as follows: female $nonA^{diss}$ *f/* $nonA^{diss}$ *f; In(2LR)O, Cy/Sco* were crossed to *In(1)FM7/Y ; transgene/In(2LR)O, Cy* males to produce a $nonA^{diss}$ *f/In(1)FM7/Y; transgene/In(2LR)O, Cy* strain. $nonA^{diss}$, *f; KpnGAL4/In(2LR)O, Cy* males were crossed to $nonA^{diss}$ *f/* $nonA^{diss}$ *f; UAS-nonA/In(2LR)O, Cy* females to obtain the $nonA^{diss}$ *f/Y; KpnGAL4/UAS-nonA* males.

Walking optomotor test: The optomotor response was tested following the method described by Burnet and Beck (1968). Flies 3–8 days old were dark adapted for ~4 hr in food vials. Each fly was tested individually for its turning behavior in a moving visual field. This was created using a rotating Plexiglass drum (diameter 8 cm; height 9 cm) that had alternating black and white vertical stripes. The stripes subtended an angle of 12.4°. The drum was constantly rotated at 30 rpm. Each fly was placed in the middle arm of a T-shaped glass tube. This arm was painted black, so that the fly was forced to walk out into a choice point where it could turn into the right or the left arm. To test whether the turning behavior corresponded to the moving environment, the tube was placed in the middle of the rotating drum. A fly produced a correct response every time it turned out of the black arm in the same direction as the rotating stripes. Canton-S and $nonA^{diss}$ b males were used as positive and negative controls, respectively. For each genotype, at least 10 individuals were tested. Each fly was given 10 trials, and each time the rotating direction of the stripes was changed. A desk lamp (60 W) was placed above the drum to illuminate in a uniform way the center of the cylinder. All tests were performed at room temperature (22°). The significance of the difference between genotypes was determined by an ANOVA test and the Tukey-Kramer *a posteriori* test by using Statistica Statsoft 3.0 for Macintosh.

Electroretinograms: ERGs were recorded from adult flies

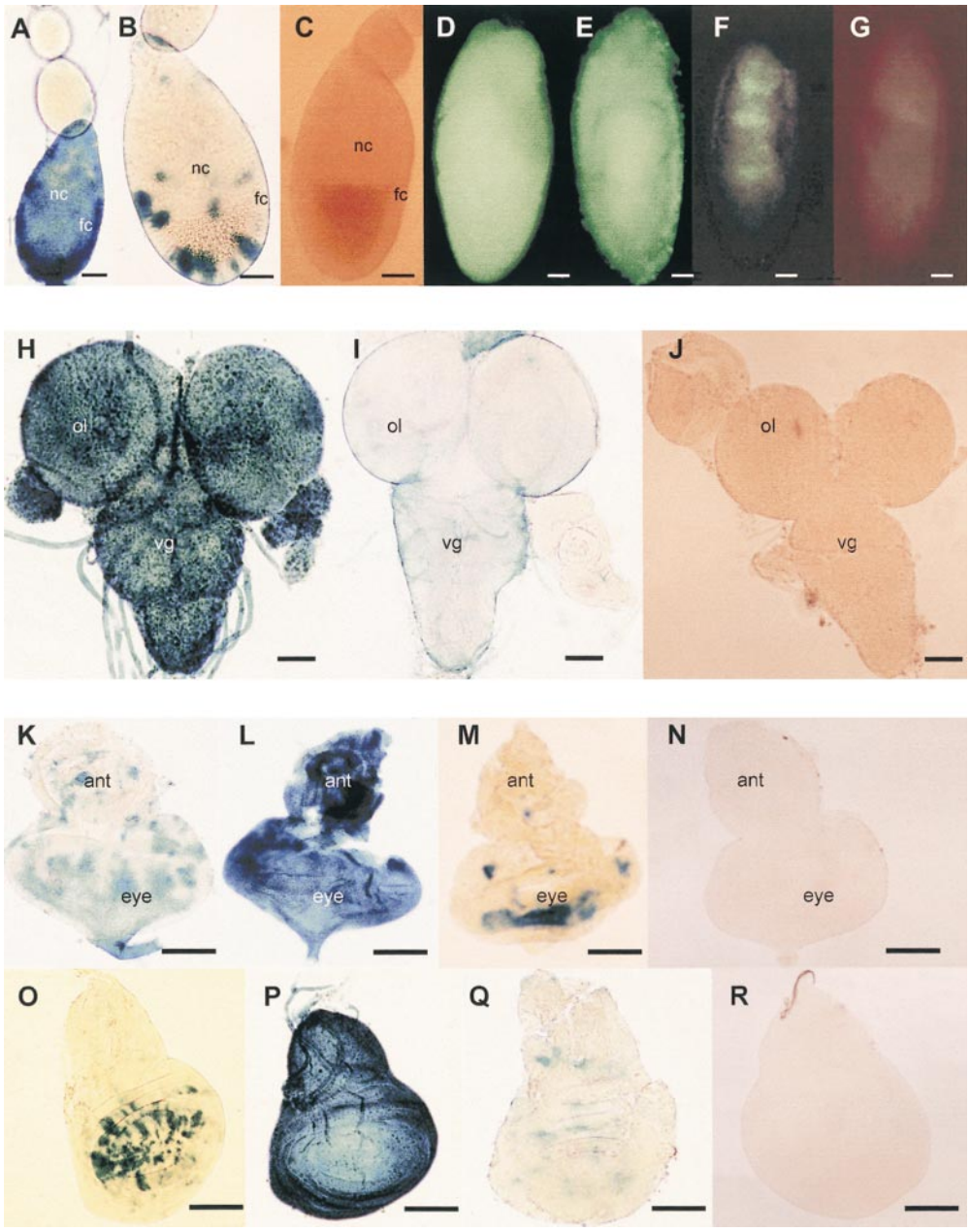

FIGURE 2.—Expression patterns of NONA in wild-type (Canton-S) and transgenic flies using anti-NONA antibodies, anti-β-gal antibodies, and X-gal staining (see text). Bars: A, 20 μm; B and C, 50 μm; D–G, 25 μm; H–J, 10 μm; K–R, 40 μm; S–Y, 100 μm. The acronym *"KpnX"* refers to flies carrying both *KpnGAL4* and *UAS-lacZ* transgenes. (A) β-Gal expression in *Kpn1* female ovaries. Activity was observed in the follicle epithelium and nurse cells. A similar expression pattern was observed in *Kpn3*, *Kpn4*, and *Kpn5* female ovaries. fc, follicle epithelium; nc, nurse cells. (B) A weaker β-gal signal, restricted to the follicle epithelium, was observed in *Kpn7* developing oocytes. (C) Control β-gal distribution pattern in a *UAS-lacZ* female ovary. (D) Localization of NONA protein with an anti-NONA antibody in a wild-type embryo at developmental stage 11. (E) Anti-β-galactosidase antibody localization of β-gal in a *Kpn1* transgenic embryo (stage 11). Similar profiles of expression were observed in *Kpn3*, *Kpn4*, and *Kpn5* embryos, while significantly weaker β-gal expression (F) was observed in *Kpn7* embryos (stage 11). (G) β-Gal pattern of expression in a *UAS-lacZ* control transgenic embryo at developmental stage 9. (H) β-Gal expression in a *Kpn1* third-instar larval brain. Similar profiles of expression were observed in *Kpn3*, *Kpn4*, and *Kpn5* third-instar larval brains. vg, ventral ganglion; ol, optic lobes. (I) A weaker β-gal expression was observed in *Kpn7* third-instar larval brains. (J) Control β-gal expression pattern in a third-instar *UAS-lacZ* larval brain. (K) β-Gal expression in the eye-antennal imaginal disc of a *Kpn1* third-instar larva. eye, eye; ant, antenna. (L) Significantly higher β-gal expression was observed in *Kpn3* eye-antennal imaginal discs. A similarly high expression was observed in *Kpn4* and *Kpn5* third-instar eye-antennal imaginal discs. (M) β-Gal expression in the eye-antennal imaginal disc of a *Kpn7* third-instar larva. β-Gal activity is here reduced and restricted to the disc posterior area. (N) A control β-gal expression pattern in a third-instar *UAS-lacZ* larval eye-antennal imaginal disc. (O) β-Gal expression in a wing imaginal disc of a *Kpn1* third-instar larva. (P) β-Gal expression in a wing imaginal disc of a *Kpn3* third-instar larva. *Kpn3*, *Kpn4*, and *Kpn5* third-instar larvae wing imaginal discs had a similar expression profile and showed more extensive β-gal expression than *Kpn1*. (Q) A significant reduction in expression was observed in *Kpn7* compared to *Kpn1* wing discs. (R) β-Gal expression in a control *UAS-lacZ* wing disc. (S) NONA protein localization, detected by anti-NONA antibody, in a frozen section (head and thorax) of a wild-type adult. ey, eye; la, lamina; me, medulla; lo, lobula; lp, lobula plate; mu, thoracic muscles. (T) β-Gal expression in head and thorax of *Kpn3* transgenic fly. A similar expression pattern was observed in *Kpn1* flies. (U) β-Gal expression in head and thorax of *Kpn4* transgenic fly. A significant increase in β-gal expression was observed in the thoracic muscles with respect to that of *Kpn1* and *Kpn3* while the β-gal expression in the head was similar to that of *Kpn1* and *Kpn3*. (V) β-Gal expression in a control *UAS-lacZ* adult fly. ey, eye; ol, optic lobe; mu, thoracic muscles. (W) β-Gal expression in a horizontal section through the head of an adult *Kpn1* transgenic fly. ey, eye; la, lamina; me, medulla; lb, lobula; lp, lobula plate. A similar expression pattern was observed in *Kpn3*, *Kpn4*, and (X) *Kpn5* adult heads. (Y) Reduced β-gal expression in a *Kpn7* head.

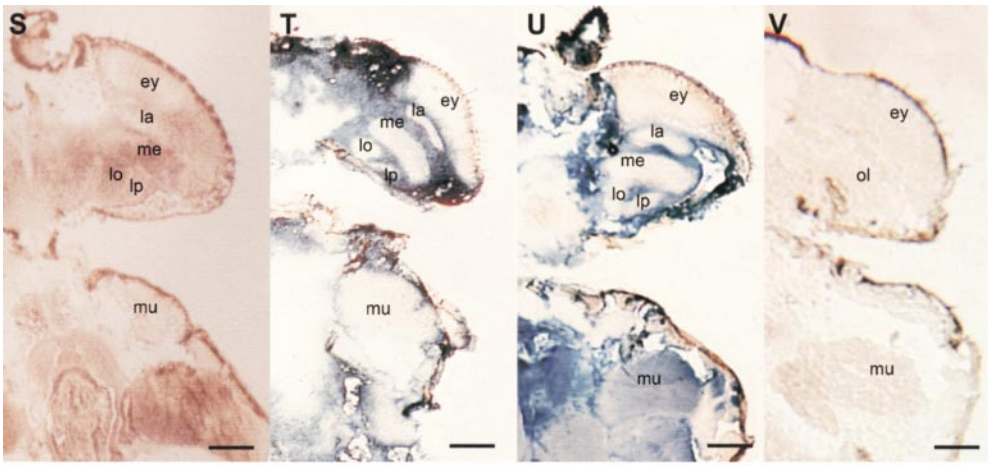

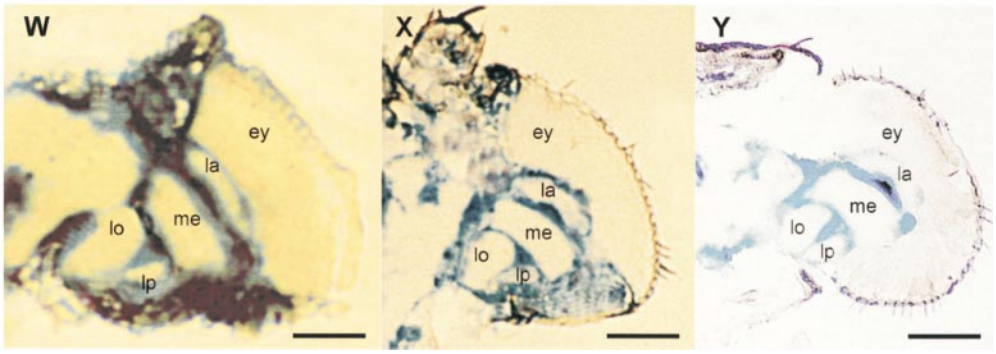

FIGURE 2.—*Continued.*

(male and female Canton-S, *nonA*^{diss} and *Kpn1-7GAL4/UAS-nonA* transgenic flies) using conventional electrophysiological techniques exactly as described in CAMPESAN *et al.* (2001, accompanying article).

Courtship song: Courtship songs were recorded as described in RITCHIE and KYRIACOU (1994). Briefly, ~10–15 min of song were recorded from the relevant 3–5-day-old male in the presence of a 1-day-old virgin female using a specially constructed electret condenser microphone (RITCHIE and KYRIACOU 1994). The songs were recorded onto magnetic tape, filtered below 100 Hz and above 1000 Hz, and digitized with a CED (Cambridge, UK) analogue to digital converter. The mean value of cycles per pulse (CPP) for the first pulse from each song train was calculated using only song trains that had more than five pulses. A large number of song trains from each male were considered, and this CPP measure distinguishes clearly the mutant *nonA*^{diss} phenotype (CPP > 2) from the wild type (CPP < 1.5, see RESULTS). CPP was measured automatically by Spike2 (CED) software after setting a threshold level above and below any noise in the recording (RITCHIE and KYRIACOU 1994).

RESULTS

Developmental expression: For each *Kpn1-7GAL4* construct, the β-galactosidase distribution patterns were analyzed at various developmental stages in different transgenic lines to reduce the possibility of expression artefacts due to position effects. It became clear early on that *UAS-lacZ* lines 1026 and 1027 gave almost identical expression levels, while line 1025 always gave lower levels compared to the others (data not shown). Consequently, only the results based on *UAS-lacZ* line 1026 are presented throughout this section.

Ovaries: Figure 2A shows the β-gal expression in the *Kpn1GAL4/UAS-lacZ* female ovary. Activity was observed in the follicle epithelium and nurse cells, and this pattern was similar to that of the NONA protein in wild-type flies, as reported by FRASH and SAUMWEBER (1989) and RENDAHL *et al.* (1992). A similar expression pattern was observed in *Kpn3-*, *Kpn4-*, and *Kpn5GAL4/UAS-lacZ* female ovaries. A weak β-gal signal was observed in the *Kpn7GAL4/UAS-lacZ* developing oocyte, which showed some punctate staining at the level of the follicle epithelium (Figure 2B). Figure 2C shows an absence of β-gal expression in a control *UAS-lacZ* female ovary.

Embryos: Figure 2D shows the localization of NONA protein, detected with an anti-NONA antibody in a wild-type (Canton-S) embryo at developmental stage 11: an ubiquitous distribution of NONA in all the embryonic tissues can be seen. All *Kpn1-*, *Kpn3-*, *Kpn4-*, and *Kpn5GAL4/UAS-lacZ* transgenic embryos show a very similar β-gal distribution profile to the NONA patterns in the wild-type controls (Figure 2E), except for one of the four *Kpn4GAL4* lines (5C), which never presented any expression at all (data not shown). In contrast, anti-β-gal staining in the *Kpn7GAL4/UAS-lacZ* embryos was much weaker (Figure 2F) if compared with the NONA

staining in the wild type or the levels of expression in all the other *KpnGAL4/UAS-lacZ* embryos. Consequently, there appears to be an enhancer of embryonic expression at least in the region between Kpn5 and Kpn7 (−223 to −673 bp from initiating *nonA* methionine codon) Figure 2G shows control β-gal distribution pattern in a *UAS-lacZ* transgenic embryo at developmental stage 9.

Larvae: β-Gal in the third instar larval brain of *Kpn1-*, *Kpn3-*, *Kpn4-*, and *Kpn5GAL4/UAS-lacZ* transformants was expressed both in the optic lobes and ventral ganglia (Figure 2H). No detectable differences in expression levels between the different *Kpn1-5* fragments were observed, and the β-gal distribution pattern was similar to that of NONA protein reported in the wild-type larval brain (Rendahl *et al.* 1992). However, in the larval brain of *Kpn7GAL4/UAS-lacZ* flies the β-gal activity was generally weak, both in the optic lobes and in the ventral ganglion (Figure 2I). Figure 2J shows a control β-gal distribution pattern in a third-instar *UAS-lacZ* larval brain.

Imaginal discs: The β-gal expression in the eye-antennal imaginal discs of *Kpn1GAL4/UAS-lacZ* third-instar larvae was mainly localized in the region that will develop into the photoreceptor cells of the adult eye (Figure 2K). In the eye-antennal discs of *Kpn3-*, *Kpn4-*, and *Kpn5GAL4/UAS-lacZ* third-instar larvae, the β-gal activity was present not only in the photoreceptor region but also in the part that will develop into the antenna (Figure 2L). Figure 2M shows an eye-antennal imaginal disc of a *Kpn7GAL4/UAS-lacZ* transgenic larva, in which the β-gal activity was significantly reduced compared to the other transgenics and restricted to the most posterior area that will form the adult eye. Figure 2N shows a control β-gal distribution pattern in an *UAS-lacZ* eye-antennal imaginal disc from a third-instar larva. Thus the distal fragment appears to have silencers that downregulate *nonA* expression in the antennal region of the disk.

The β-gal expression in the wing imaginal discs of *Kpn1GAL4/UAS-lacZ* third-instar larvae was predominantly localized in the region that will develop into the epithelial layer (Figure 2O). In the corresponding discs of *Kpn3-*, *Kpn4-*, and *Kpn5GAL4/UAS-lacZ* larvae, β-gal was expressed more extensively, both in the epithelial region and in the portion that will originate part of the thoracic cuticle, suggesting the existence of silencers in the distal fragment (Figure 2P). In the wing discs of *Kpn7GAL4/UAS-lacZ* larvae, the β-gal activity was significantly reduced compared to that of the other transformants (Figure 2Q). Again, the distal fragment −1198 to −1827 bp appears to carry silencers for the expression of imaginal disc tissue. Figure 2R shows a control β-gal distribution pattern in a *UAS-lacZ* wing disc.

Adult: Figure 2S shows the wild-type localization of NONA protein, detected by using an anti-NONA antibody in a frozen section of an adult fly. Antigen was seen in most cells of all tissues examined including photoreceptors, lamina, medulla, lobula and lobula plate of the optic lobe, the central brain, and the thoracic ganglia. Also thoracic muscles and the gut were stained. The β-gal distribution pattern in the head of *Kpn1-*, *Kpn3-*, *Kpn4-*, and *Kpn5GAL4/UAS-lacZ* transgenic flies was similar to that of the NONA protein in wild-type flies (Figures 2W, 2T, 2U, and 2X, respectively). Figure 2Y shows a head section of *Kpn7GAL4/UAS-lacZ* transgenic flies with the β-gal expression significantly reduced. A weak activity was found in the central brain, in the lobula, in the lobula plate, and in the medulla, whereas little expression was observed in the lamina and none in the photoreceptor cells. The β-gal expression pattern in the thorax of *Kpn1-* and *Kpn3GAL4/UAS-lacZ* individuals was similar to that reported for NONA protein in wild type (Figure 2T).

Interestingly, in the thoracic muscles of *Kpn4GAL4/UAS-lacZ* adults we observed an extensive increase in β-gal expression level (Figure 2U), suggesting the elimination of an adult muscle silencing factor(s) in the 344-bp fragment that delimits the *Kpn3GAL4* from the *Kpn4GAL4* construct. The β-gal expression level in the adult thoracic muscles of *Kpn5GAL4/UAS-lacZ* flies in two independently derived lines (15A and 41B) was different. Whereas 15A flies showed high β-gal levels, estimated to lie between those of *Kpn1-* and *Kpn4GAL4/UAS-lacZ*, the 41B flies showed no β-gal expression at all, indicating a position effect. The β-gal pattern in the thorax of *Kpn7GAL4/UAS-lacZ* flies was significantly reduced compared to all the other *KpnGAL4/UAS-lacZ* lines, and weak expression was observed in the thoracic ganglia, but none in muscle cells. Figure 2V shows a control β-gal distribution pattern in a section of an *UAS-lacZ* adult.

Optomotor test: Confronted with a binary choice as to whether to follow the direction of the stripe movement, $nonA^{diss}$ individuals turn at random, giving a mean value for the genotype of 50.5%. Canton-S males turn in the direction of the movement >80% of the time (Figure 3). Hemizygous $nonA^{diss}$ males carrying the five different *KpnGAL4* and *UAS-nonA* transgenes gave graded responses that reflected the amount of *nonA* promoter material carried in the insert—from 72.1% correct responses in *Kpn1* to 50.2% in *Kpn7GAL4/UAS-nonA* flies (Figure 3). ANOVA gave highly significant differences between these values ($F = 28.29$; $P = 0.0001$). There are no significant differences (Tukey-Kramer test) between the wild-type (Canton-S) and *Kpn1-*, *Kpn3-*, and *Kpn4-GAL4/UAS-nonA* genotypes. Similarly, the mean value obtained for *Kpn7GAL4/UAS-nonA* was not significantly different from that of $nonA^{diss}$ negative controls. *Kpn5-GAL4/UAS-nonA* has a significantly poorer response compared to wild type (Canton-S) and *Kpn1GAL4/UAS-nonA*, but significantly higher than $nonA^{diss}$ and *Kpn7-GAL4/UAS-nonA* (all $P < 0.001$). These results suggest that enhancers for the optomotor response must lie in

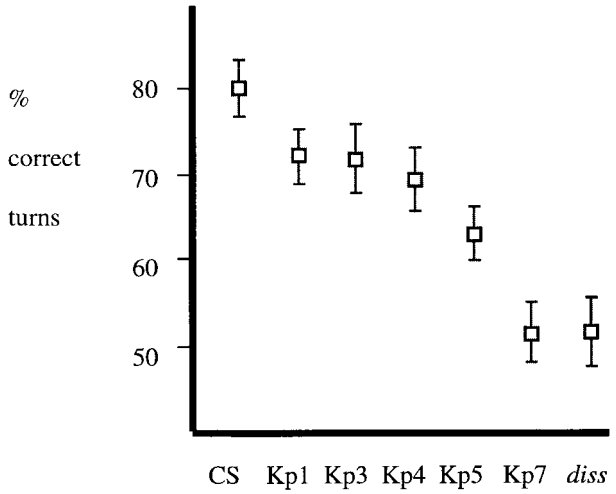

FIGURE 3.—Optomotor response of Canton-S (CS), *nonA*^{diss} (*diss*), and hemizygous *nonA*^{diss} males carrying *KpnGAL4* and *UAS-nonA* transgenes (Kp). The mean optomotor response of single male flies is expressed as percentage of turns in direction of the stripe movement (correct turns, see MATERIALS AND METHODS). From 20 to 70 flies were analyzed for each genotype. Mean values plus SDs are given.

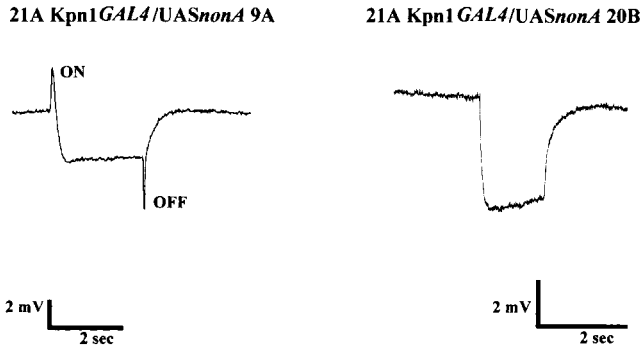

FIGURE 4.—ERGs from transgenic males carrying the 21A *Kpn1GAL4* and 9A *UAS-lacZ* transgenes or the same *Kpn1GAL4* insert and *UAS-lacZ* 20B (see Table 1). No rescue of ERG was observed in any of the other transgenic genotypes, which all showed ERGs identical to those of *nonA*^{diss} mutants (see also Table 1).

the regions between the *Kpn4*, *Kpn5*, and *Kpn7* fragments.

ERGs: As reported in Table 1, almost all the transgenic individuals tested showed an ERG response characterized only by the sustained component and lacking the transient light-on and light-off components. Only in transgenic individuals with the 21A *Kpn1GAL4/UAS-nonA* 9A genotype was a wild-type ERG response observed in five out of six flies (Figure 4). Surprisingly, the light-on and light-off transient amplitudes in these individuals were significantly higher than those observed in wild-type (Canton-S) individuals ($P < 0.001$; Table 1).

Courtship song: Between three and six songs were analyzed for various lines of *Kpn1-*, *Kpn3-*, *Kpn4-*, and *Kpn7GAL4/UAS-nonA* on a *nonA*^{diss} background. This included two lines that carried only the *UAS-nonA* transgene and the *235R11 nonA*$^{+}$ control transformants (see

TABLE 1

ERG response in wild-type (Canton-S) and *Kpn1-7GAL4/UAS-nonA* transgenic flies

Genotype	*N*	+	Light-on	Light-off	−
30G *Kpn1/UAS-nonA* 20B	7	0			7
30G *Kpn1/UAS-nonA* 9A	10	0			10
21A *Kpn1/UAS-nonA* 20B	5	0			5
21A *Kpn1/UAS-nonA* 9A	6	5	3.8 ± 0.2 (24)	5.0 ± 0.9 (22)	1
28A *Kpn1/UAS-nonA* 20B	6	0			6
28A *Kpn1/UAS-nonA* 9A	3	0			3
15A *Kpn3/UAS-nonA* 20B	7	0			7
15A *Kpn3/UAS-nonA* 9A	10	0			10
18D *Kpn4/UAS-nonA* 20B	4	0			4
18D *Kpn4/UAS-nonA* 9A	4	0			4
41B *Kpn5/UAS-nonA* 20B	8	0			8
41B *Kpn5/UAS-nonA* 9A	6	0			6
15B *Kpn5/UAS-nonA* 20B	1	0			1
15B *Kpn5/UAS-nonA* 9A	10	0			10
34A *Kpn7/UAS-nonA* 20B	2	0			2
34A *Kpn7/UAS-nonA* 9A	2	0			2
24B *Kpn7/UAS-nonA* 20B	3	0			3
24B *Kpn7/UAS-nonA* 9A	3	0			3
Canton-S	4	4	2.8 ± 1.0 (16)	2.4 ± 1.2 (14)	0

N, number of flies tested; +, wild-type ERGs (with light-on and light-off transients); −, mutant ERGs (without light-on and light-off transients). Mean, SD, and number (parentheses) of light-on and light-off amplitudes (mV) in Canton-S and in rescued 21A *Kpn1/UAS-nonA* 9A transgenic flies are also reported.

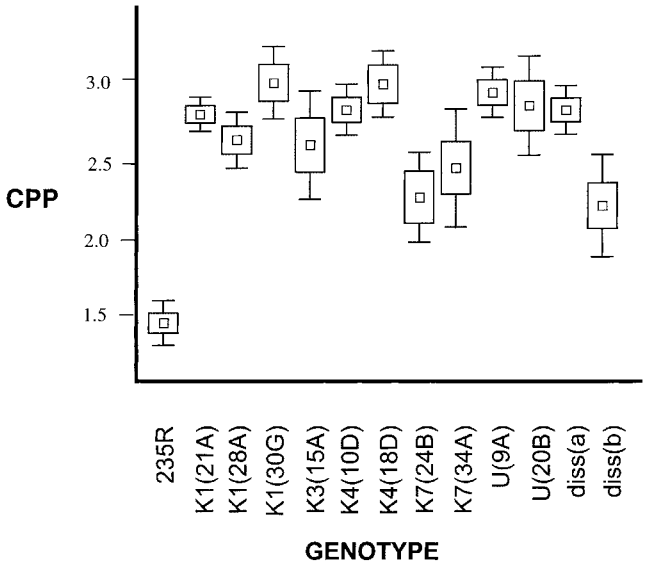

FIGURE 5.—Mean CPP scores for courtship song. SEMs and SDs are also shown in the box-and-whiskers plot. "235R" represents the wild-type *nonA* transformants 235R11 (see MATERIALS AND METHODS), the prefix "K" represents the promoter-*GAL4* fusions, the prefix "U" the two *UAS-nonA* lines, and diss(a) and diss(b) represent the two groups of $nonA^{diss}$ males (see text).

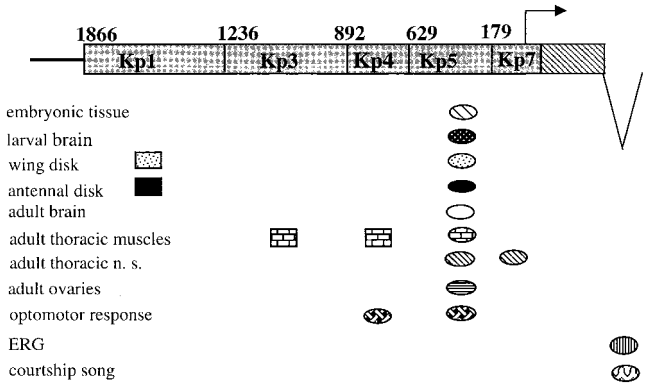

FIGURE 6.—Cartoon depicting the regulatory region of *nonA*. The first intron in the coding sequence is depicted as a "V." The first *nonA* exon is shown as a textured box and the 5′ region is shown in gray, marked with the various *Kpn* deletions (labeled "Kp"). The amount of 5′ material in base pairs is given for each construct. Ovals are placed within those *Kpn* fragments that enhance expression of a *UAS-lacZ* transgene, and squares represent fragments that downregulate *nonA* expression. The ovals in the Kp7 region represent the residual expression for the relevant phenotypes seen in *Kpn7GAL4/UAS-lacZ* flies. The *dGpi1* intron/exon structure is superimposed above the *nonA* regulatory region. The first exon of *dGpi1* lies at position −2372 bp upstream of the initiating *nonA* methionine codon (CAMPESAN *et al.* 2001, accompanying article). The 3′ end of each *KpnGAL4* transgene lies 44 bp upstream of the *nonA* initiating methionine codon (CAMPESAN *et al.* 2001, accompanying article).

MATERIALS AND METHODS). The two groups of mutant $nonA^{diss}$ songs (a and b, see MATERIALS AND METHODS) were also recorded. We observed from preliminary analyses that in both these mutant lines, the average CPP value for the very first pulse in the song burst was >2. This value was thus significantly higher (see below) than the value for the *235R11* $nonA^{+}$ control transformants, which was <1.5 (see Figure 5). KULKARNI *et al.* (1988) also showed that the very first pulse of a $nonA^{diss}$ mutant train also had a higher CPP value than that of the (non-transformant) wild-type song. However, subsequent studies have used the significant and steady increase in CPP, which is observed during a $nonA^{diss}$ mutant song train and which is not observed in the wild-type songs, to discriminate between the two genotypes (*e.g.*, RENDAHL *et al.* 1992, 1996). We avoided this extremely labor-intensive approach, which requires logging all the pulses in each train, and replaced it by simply scoring the relevant pulse characteristics from the very first pulse of each train. This modified and shortened procedure revealed that neither the *KpnGAL4/UAS-nonA* nor the *UAS-nonA* transformants showed any evidence for rescue of the $nonA^{diss}$ song defect as measured by the high mean CPP values of the very first pulse in a train that ranged from 2.2 to 3.0 (Figure 5). The two $nonA^{diss}$ lines also showed high CPP values as expected from the preliminary results. In contrast, the songs of *235R11* transformants, which carry the transgene that rescues all mutant phenotypes of $nonA^{diss}$, gave a mean CPP value of <1.5 (Figure 5). ANOVA gave a significant *F*-ratio ($F = 13.2$, d.f. 12, $P \ll 0.00001$), due mainly to the difference between *235R11* and the other groups. *Post hoc* tests also revealed a few marginal significant differences between some of the other groups. We conclude that the 5′ region of *nonA* does not carry sequences that permit the normal expression of the wild-type song phenotype.

Does the *Kpn1GAL4* fragment rescue *l(1)i19e* lethality? The 5′ end of the large *Kpn1GAL4* fragment encodes the sequences of *dGpi1* from residue 149 onward (CAMPESAN *et al.* 2001, accompanying article). The *dGpi1* transcription unit almost certainly corresponds to *l(1)i19e*, so the *Kpn1GAL4* fragment should not rescue the *l(1)i19e* mutation because the N-terminal third of the dGPI1 will be absent. Heterozygous *l(1)i19e/In(1) FM7, w* females were crossed to *X/Y; Kpn1GAL4/*balancer males. If the *Kpn1GAL4* fragment rescues *l(1)i19e* lethality, there should be non-*In(1) FM7, w* males among the progeny. We obtained 317 F_1 males carrying *In(1) FM7, w* but not a single *l(1)i19e/Y; Kpn1GAL4/+* male.

DISCUSSION

An overview of the spatial distribution of putative regulatory regions within the *nonA* promoter is shown in Figure 6. It is clear that the 451-bp fragment between *Kpn5* and *Kpn7GAL4* contains upregulating elements for all of the anatomical and one of the behavioral phenotypes. Residual contributions toward expression

in the larval brain, eye and antennal discs, and adult CNS can be detected with the *Kpn7GAL4* transgene. The restricted eye-antennal disc expression driven from this 5′ fragment is limited to differentiating cells. The posterior ommatidia of the eye-antennal disc are formed first, and the anterior last (Lawrence 1992), so the proximal element could guarantee the early expression of *nonA* in these developing photoreceptors. More complex patterns of regulation are found for the eye-antennal and wing imaginal discs. In the more distal region located between *Kpn1GAL4* and *Kpn3GAL4*, silencers appear to be present whose elimination leads to increased expression in these imaginal discs (Figure 6). In the adult, the *Kpn7* region also drives low levels of transgene expression in the adult CNS. Moreover, silencing signals that downregulate expression in the adult thoracic muscles appear to be localized in the region present in *Kpn3* but absent in *Kpn5GAL4*. Finally, sequences that drive *nonA* expression in the follicle epithelium and nurse cells of the female ovary are again localized in the proximal 450-bp region (between *Kpn5GAL4* and *Kpn7GAL4*).

The data obtained from the walking optomotor test for *Kpn1*-, *Kpn3*-, and *Kpn4GAL4/UAS-nonA* flies that carried the larger promoter fragments revealed that the proportion of correct turning responses was lower, but not significantly different from the wild-type control. The optomotor behavior of *Kpn5GAL4* flies was significantly poorer, but we did not see a correlated change in reporter gene activity in the optic lobes, even though a relationship between NONA protein levels and the optomotor phenotype has been reported (Rendahl *et al.* 1992; Stanewsky *et al.* 1993). Only in the *Kpn7GAL4* transformants was there an association between the reduced *lacZ* reporter gene activity in the optic regions, with the further deterioration in optomotor performance. The significant decrease in the optomotor values of *Kpn5* and *Kpn7* transformants highlights the role of the 613-bp proximal element located between *Kpn4* and *Kpn7GAL4*, which we presume may determine *nonA* levels in the lobula plate, the region in the optic lobes believed to play an important role in the control of the optomotor responses (Heisenberg *et al.* 1978).

Given the results of the optomotor response, it is perhaps surprising that only flies from line 21A *Kpn1GAL4/UAS-nonA* 9A showed rescue of the ERG. The progressive deletion of the *nonA* promoter region clearly has different effects on the two visual phenotypes. However, mutants defective in the ERG, but not in optomotor responses, have been described (Heisenberg 1972) and various *nonA* transformants show a similar dissociation of the two visual phenotypes (Rendahl *et al.* 1992). Thus the neural foci generating the ERG transients that are localized in the synapses within the first optic ganglion (lamina) are different from those that mediate the optomotor response (Heisenberg *et al.* 1978; Coombe 1986). Because the genomic *235R11* transgene rescues *nonA* mutant ERGs (Rendahl *et al.* 1992, 1996), we suspect that the introns that are absent in the *UAS-nonA* cDNA may be carrying enhancers for this phenotype. Intronic enhancers are a common feature of Drosophila genes. For example, a 32-bp region within the second intron of *proboscipedia* acts as a labial disk enhancer (Kapoun and Kaufman 1995), whereas a 212-bp intron region within *eyeless* acts as an enhancer for both embryonic eye promordia and in the eye disks (Hauck *et al.* 1999). The rescue of ERGs in 21A *Kpn1GAL4/UAS-nonA* 9A individuals could reflect a position effect in which the *Kpn1GAL4* transgene has come under the control of a local visual system "upregulating" enhancer. This view is supported by the peculiarly high-amplitude light-on and light-off transients observed in these rescued individuals when compared with the corresponding values in the control flies. However, it is still difficult to explain why the same *Kpn1GAL4* transgene, when crossed to other independent *UAS-nonA* inserts, fails to rescue the ERG without advocating a peculiar interaction specific to those two lines.

Unlike the ERG results, where one line did rescue the mutant phenotype, no rescue of normal courtship song pulses was obtained even in the *Kpn1GAL4* lines. This is unlikely to be due to the insert positions of all of these lines, so an explanation must be sought elsewhere. Once again we are forced to conclude that the introns of *nonA* may contain elements for enhancing the song phenotype. A *hsp-nonA* (cDNA) transgene rescues both song and visual defects of $nonA^{diss}$ mutants, even when the transgene is activated only in adulthood (Rendahl and Hall 1996). In the rescued transformants, the levels of heat-shock NONA detected by Western blots were almost twice those of wild type (Rendahl and Hall 1996). Therefore the high, promiscuous levels of NONA expression from the heat-shock promoter may have compensated for any enhancement problems stemming from the absence of introns. The first large >1.2-kb *nonA* intron in *D. melanogaster* reveals many putative binding sites for transcription factors that are detected by various algorithms (see Campesan *et al.* 2001, accompanying article; S. Campesan, unpublished results). Comparisons with the much larger 2.4-kb *D. virilis* first intron reveal conservation of a number of transcription factor sites including those for Even-skipped, Fushi-tarazu, Giant, Zerknullt, and Zeste (S. Campesan, unpublished results). In the 40–60 million years since these two species had a common ancestor, the neutral nucleotide substitution rate would have eliminated any sequence similarity that is not under selection (Moriyama 1987; Moriyama and Gojobori 1992; Schlotterer *et al.* 1994). Consequently, conservation of these putative intronic binding sites between the two species may represent functional regulatory regions.

The recently identified *dGpi1* gene overlaps with a large fraction of the *nonA* 5′ sequences and almost cer-

tainly corresponds to *l(1)i19e* (Campesan *et al.* 2001, accompanying article). We could not rescue *l(1)i19e* lethality by crossing in the largest *Kpn1GAL4* fragment, and so our results are not inconsistent with this view. From Figure 6 it can be observed that for every phenotype examined, anatomical or behavioral, upregulators for *nonA* expression are to be found in the region between the 5′ ends of fragments *Kpn5* and *Kpn7*. The transcription unit for *dGpi1* ends in this region, 424 bp upstream of the initiating methionine of *nonA* in *D. melanogaster* (Campesan *et al.* 2001, accompanying article). This leaves ~200 bp within this *Kpn5–7* region that is downstream of the *dGpi1* transcription unit and upstream of the *Kpn7* fragment, where we might predict that the majority of the enhancer elements might lie and thus not overlap with *dGpi1* sequences. Within this intergenic region are found a putative Broad-Complex, Kruppel, and a heat-shock factor binding site (Campesan *et al.* 2001, accompanying article). However, the distal part of the *Kpn5* fragment that does correspond to *dGpi1* sequences (from the end of exon 7; see Figure 6) has a much larger number of putative transcription factor binding elements including Deformed, Antennapedia, Dorsal, and Broad-Complex (see Figure 6 in Campesan *et al.* 2001, accompanying article). The silencers of *nonA* expression for the wing and antennal disks and adult thoracic muscles, plus enhancers for the optomotor response, must lie within this region of the *dGpi1* transcription unit. Future work will aim at elucidating the relative roles of the intergenic region *vs.* the *dGpi1* sequence in their contribution to *nonA* regulation in this apparently congested area that defines *Kpn5* from *Kpn7*.

To our knowledge this is the first time that coding sequences of a gene have been implicated as regulatory elements for its neighbor, at least in Drosophila. Overlapping genes are common in prokaryotes because of the constraints imposed by their small genome sizes. They are also found in eukaryotes and include genes inserted into the introns of other genes, genes that share a bidirectional promoter, 3′ overlapping genes in which 3′ exons are encoded by the same DNA fragment, and genes that share regulatory regions (reviewed in Bonnelye and Laudet 1994). In Drosophila, the *janusB* (*janB*) transcription unit is encoded within the 3′ untranslated exon of the adjacent *janA* gene (Yanicostas and Lepesant 1990). Promoter-reporter *janB* fusions reveal that the presence of the *janA* 3′ sequences leads to reduced expression of the hybrid mRNA during spermatogenesis, suggesting that transcriptional interference may downregulate *janB* when both genes are being transcribed (Yanicostas and Lepesant 1990).

It is therefore intriguing that all the sequences that downregulate expression of *nonA* in the wing and antennal disks and in the adult thoracic muscles are to be found embedded in the *dGpi1* transcription unit. Study of the temporal and spatial expression patterns of *dGpi1* could illuminate the possibility of transcriptional interference between these two adjacent genes. In any case, the implications for the evolution of these regulatory sequences that are present within *dGpi1* and in the intergenic spacer between *dGpi1* and *nonA* have been explored by Campesan *et al.* (2001, accompanying article). These authors observed that putative binding sequences for transcription factors in the intergenic region showed a significant excess of fixed changes relative to polymorphisms compared to sites within *dGpi1* sequences, suggesting a selective constraint within the latter region.

In conclusion, the promoter fragment we have studied contains sequences that enhance and silence developmental and behavioral expression of *nonA*. All of the silencers are found within the *dGpi1* transcription unit, suggesting a novel type of regulation of a downstream gene by the coding regions of its neighbor. We further suggest that there may be other regulatory sequences relevant for the ERG and courtship song phenotypes, and these may be located within the four introns of *nonA* that range from the smallest, 80 bp, to the largest, >1.2 kb (Jones and Rubin 1990). If the introns are not involved, then it would suggest that either the absence of the 45 bp of untranslated material in the *nonA* first exon may be responsible or that the GAL4 *trans*-activation paradigm interferes with the normal expression of *nonA*. This could happen if spatial relationships between enhancers in the 5′ region and within the *nonA* transcription unit itself were critical for some features of *nonA* expression. There is some evidence that using promoter GAL4 fusions can generate expression patterns that are not usually observed with the native sequences. For example, fusions of the *timeless (tim)* promoter to GAL4 produced ectopic expression of UAS-GFP in larval brain cells that were not observed using TIM immunohistochemistry (Emery *et al.* 1998). Such additional ectopic patterns might be expected if GAL4 stability is greater than that of the native protein that it replaces.

We thank Nicolò Osterwalder and Helen Roe for technical support. We acknowledge the Ministero per l'Università e la Ricerca Scientifica e Tecnologica (MURST) for research grants to R.C. and A.M., a MURST studentship for a "dottorato di ricerca" to F.S., an ERASMUS studentship to F.S., a Human Frontiers Science Programme grant to C.P.K., a CEC predoctoral fellowship for S.C., and a Biotechnology and Biological Sciences Research Council studentship to M.C.

LITERATURE CITED

Besser, H. V., P. Schnabel, C. Wieland, E. Fritz, R. Stanewsky *et al.*, 1990 The puff-specific *Drosophila* protein Bj6, encoded by the gene *no-on-transientA*, shows homology to RNA-binding proteins. Chromosoma **100:** 37–47.

Bonnelye, E., and V. Laudet, 1994 Overlapping genes. M-S (Med. Sci.) **10:** 805–816.

Brand, A. H., and N. Perrimon, 1993 Targeted gene expression as a mean of altering cell fates and generating dominant phenotypes. Development **118:** 401–415.

Burnet, B., and J. Beck, 1968 Phenogenetic studies on visual acuity in *Drosophila melanogaster*. J. Insect Physiol. **57:** 855–860.

Campesan, S., D. Chalmers, F. Sandrelli, A. Megighian, A. A. Peixoto *et al.*, 2001 Comparative analysis of the *nonA* region in Drosophila identifies a highly diverged 5′ gene that may constrain *nonA* promoter evolution. Genetics **157:** 751–764.

Campos-Ortega, J. A., and V. Hartenstein, 1985 *The Embryonic Development of Drosophila melanogaster.* Springer Verlag, Berlin.

Coombe, P. E., 1986 The large monopolar cells L1 and L2 are responsible for ERG transients in *Drosophila.* J. Comp. Physiol. **159:** 655–665.

Emery, P., W. V. So, M. Kaneko, J. C. Hall and M. Rosbash, 1998 CRY, a *Drosophila* clock and light-regulated cryptochrome, is a major contributor to circadian rhythm resetting and photosensitivity. Cell **95:** 669–679.

Frash, M., and H. Saumweber, 1989 Two proteins from *Drosophila* nuclei are bound to chromatin and are detected in a series of puffs on polytene chromosomes. Chromosoma **97:** 272–281.

Fischer, J. A., E. Giniger, T. Maniatis and M. Ptashne, 1988 GAL4 activates transcription in *Drosophila.* Nature **332:** 853–856.

Gloor, G., and W. Engels, 1990 Single-fly DNA preps for PCR. *Drosophila* Inf. Newsl. **1**.

Hauck, B., W. J. Gehring and U. Walldorf, 1999 Functional analysis of an eye specific enhancer of the *eyeless* gene in *Drosophila.* Proc. Natl. Acad. Sci. USA **96:** 564–569.

Heisenberg, M., 1972 Comparative behavioral studies on two visual mutants of *Drosophila.* J. Comp. Physiol. **80:** 119–136.

Heisenberg, M., and K. G. Gotz, 1975 The use of mutations for the partial degradation of vision in *Drosophila melanogaster.* J. Comp. Physiol. **98:** 217–241.

Heisenberg, M., R. Wonneberger and R. Wolf, 1978 *Optomotor-blindH31*—a *Drosophila* mutant of the lobula plate giant neurons. J. Comp. Physiol. **124:** 287–296.

Hotta, Y., and S. Benzer, 1969 Abnormal electroretinograms in visual mutants of *Drosophila.* Nature **222:** 354–356.

Johnson, G. D., and G. M. G. Nogueira-Araujo, 1981 Simple method of reducing the fading of immunofluorescence during microscopy. J. Immunol. Methods **43:** 349–350.

Jones, K. R., and G. M. Rubin, 1990 Molecular analysis of *no-on-transient A*, a gene required for normal vision in *Drosophila.* Neuron **4:** 711–723.

Kapoun, A. M., and T. C. Kaufman, 1995 A functional analysis of 5′, intronic and promoter regions of the homeotic gene *proboscipedia* in *Drosophila melanogaster.* Development **121:** 2127–2141.

King, R. C., 1970 *Ovarian Development in Drosophila melanogaster.* Academic Press, New York.

Klemenz, R., U. Weber and W. J. Gehring, 1987 The *white* gene as a marker in a new P element vector for gene transfer in *Drosophila.* Nucleic Acids Res. **15:** 3947–3659.

Kulkarni, S. J., A. F. Steinlauf and J. C. Hall, 1988 The *dissonance* mutant of courtship song in *Drosophila melanogaster*: isolation, behavior and cytogenetics. Genetics **118:** 267–285.

Laughon, A., R. Driscoll, N. Wills and R. F. Gesteland, 1984 Identification of two proteins encoded by *Saccharomyces cerevisiae gal4* gene. Mol. Cell. Biol. **4:** 268–275.

Lawrence, P. A., 1992 *The Making of a Fly.* Blackwell Scientific Publications, Oxford.

Lindsley, D. L., and G. G. Zimm, 1992 *The Genome of Drosophila melanogaster.* Academic Press, San Diego.

Moriyama, E. N., 1987 Higher rates of nucleotide substitution in *Drosophila* than in mammals. Jpn. J. Genet. **62:** 139–147.

Moriyama, E. N., and T. Gojobori, 1992 Rates of synonymous substitution and base composition of nuclear genes in *Drosophila.* Genetics **130:** 855–864.

Pak, W. L., H. Grossfield and S. Arnold, 1970 Mutants of the visual pathway of *Drosophila melanogaster.* Nature **227:** 518–520.

Phelps, C. B., and A. H. Brand, 1998 Ectopic gene expression in *Drosophila* using GAL4 system. Methods **14:** 367–379.

Reim, I., R. Stanewsky and H. Saumweber, 1999 The puff-specific RRM protein NONA is a single stranded nucleic acid binding protein. Chromosoma **108:** 162–172.

Rendahl, K. G., and J. C. Hall, 1996 Temporally manipulated rescue of visual and courtship abnormalities caused by a *nonA* mutation in *Drosophila.* J. Neurogenet. **10:** 247–256.

Rendahl, K. G., K. R. Jones, S. J. Kulkarni, S. H. Bagully and J. C. Hall, 1992 The *dissonance* mutation at the *no-on-transient A* locus of *D. melanogaster*: genetic control of courtship song and visual behaviors by a protein with putative RNA-binding motif. J. Neurosci. **12:** 390–407.

Rendahl, K. G., N. Gaukhshteyn, D. A. Wheeler, T. A. Fry and J. C. Hall, 1996 Defects in courtship and vision caused by amino acid substitutions in a putative RNA-binding protein encoded by the *no-on-transient A (nonA)* gene of *Drosophila.* J. Neurosci. **15:** 1511–1522.

Ritchie, M. G., and C. P. Kyriacou, 1994 Genetic variability of courtship song in population of *Drosophila melanogaster.* Anim. Behav. **48:** 425–434.

Roberts, D. B., and G. N. Standen, 1998 The elements of *Drosophila* biology and genetics, pp. 1–54 in *Drosophila: A Practical Approach*, Ed. 2, edited by D. B. Roberts. IRL Press, Oxford.

Rubin, G. M., and A. C. Spradling, 1982 Genetic transformation of *Drosophila* with transposable element vectors. Science **218:** 348–353.

Sambrook, J., E. F. Fritsch and T. Maniatis, 1989 *Molecular Cloning: A Laboratory Manual*, Ed. 2. Cold Spring Harbor Laboratory Press, Cold Spring Harbor, NY.

Schlotterer, C., M. T. Hauser, A. von Haeseler and D. Tautz, 1994 Comparative evolutionary analysis of rDNA ITS regions in *Drosophila.* Mol. Biol. Evol. **11:** 513–522.

Schmidt, E. R., H. L. Keyl and T. Hankeln, 1988 *In situ* localization of two haemoglobin gene clusters in the chromosomes of 3 species of *Chironomus.* Chromosoma **96:** 353–359.

Spradling, A. C., and G. M. Rubin, 1982 Transposition of P elements into *Drosophila* germ line chromosome. Science **218:** 341–352.

Stanewsky, R., K. G. Rendhal, M. Dill and H. Saumweber, 1993 Genetic and molecular analysis of the X chromosomal region 14B17-14C4 in *Drosophila melanogaster*: loss of function in NONA, a nuclear protein common to many cell types, results in specific phyiological and behavioral defects. Genetics **135:** 419–422.

Stanewsky, R., T. A. Fry, I. Reim, H. Saumweber and J. C. Hall, 1996 Bioassaying putative RNA-binding motifs in a protein encoded by a gene that influences courtship and visually mediated behavior in *Drosophila*: *in vitro* mutagenesis of *nonA*. Genetics **143:** 259–275.

Tautz, D., and C. Pfeifle, 1989 Localization of specific RNAs in *Drosophila* embryos reveals translation control of the segmentation gene *hunchback.* Chromosoma **98:** 81–85.

Yanicostas, C., and J. M. Lepesant, 1990 Transcriptional and translational *cis*-regulatory sequences of the spermatocyte-specific *Drosophila janusB* gene are located in the 3′ exonic region of the overlapping *janusA* gene. Mol. Gen. Genet. **224:** 450–458.

Communicating editor: J. J. Loros